SUPPLEMENTARY MATERIAL

Insights into the flame transitions and flame stabilization mechanisms in a freely falling burning droplet encountering a co-flow

Gautham Vadlamudi [1], Akhil Aravind [1], and Saptarshi Basu [1,2]*

*: Corresponding author email: sbasu@iisc.ac.in

Affliations:

[1] Department of Mechanical Engineering, Indian Institute of Science, Bangalore 560012, India

[2] Interdisciplinary Centre for Energy Research (ICER), Indian Institute of Science, Bangalore 560012, India

Figure S1: The wake flame images (obtained in pendant mode during our previous experiments) obtained using a UV transparent lens: without OH* filter, DSLR (colored), and with OH* filter (OH* Chemiluminescence) [from left to right]; showing similar flame front contour for the droplet wake flame without bright sooty tip (represented by blue data points). The wake flame height vs relative velocity correlation is observed to follow a linear trend for the cases without sooty tip (blue data points), and the dotted line is the linear fit. The orange data points representing the cases with a bright sooty tip significantly deviate from the linear correlation. Hence, the sooty tip cases were not considered in the current study.
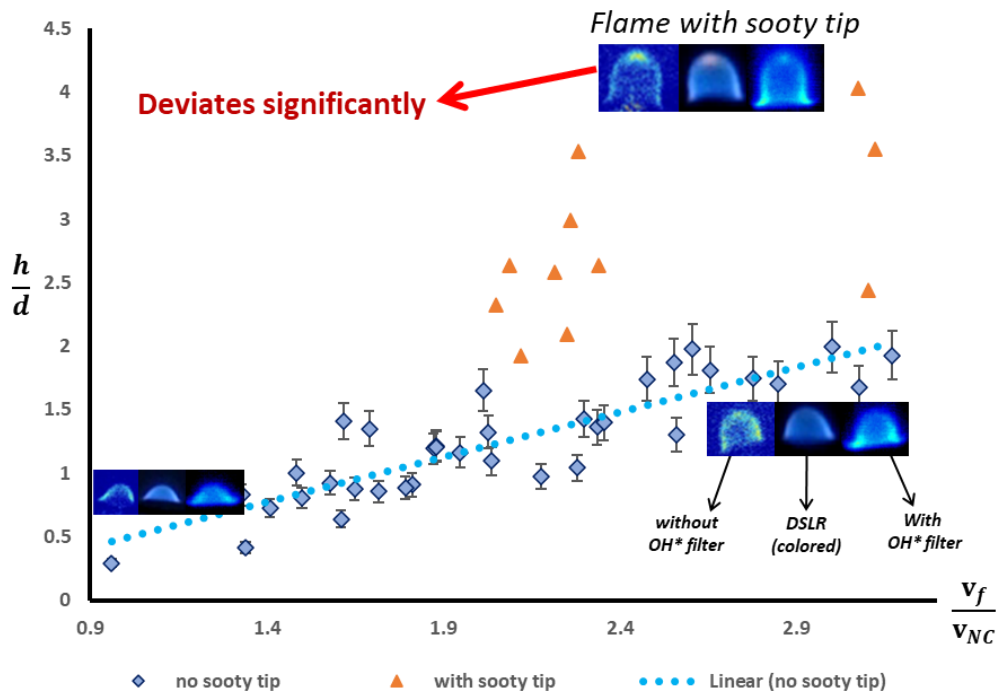
The flame imaging is done using a UV transparent lens, whose transmittance spectrum includes the range of the OH* and CH* chemiluminescence (310 nm and 431 nm, respectively). But due to the experimental limitations of the highspeed imaging of the low-intensity wake flame, OH* filter is not used alongside the UV lens for imaging.

However, this concern have been addressed in our previous studies, where the wake flame imaging is performed at low fps using an OH* filter coupled camera with simultaneous DSLR imaging for a pendant droplet flame. The burning droplet is imposed with a vertically upward external flow (similar

droplet size and flow velocity) to emulate the falling droplet. Those experiments were performed in a wide parametric space, and bright yellow tip (sooty flame) was observed to appear in a narrow range of droplet diameter and local flow velocity. For the regime with no sooty bright yellow tips, both the DSLR (colored) and OH* chemiluminescence images showed similar flame shape and height. This is also reflected in the images taken without OH* filter.

A linear correlation between the flame height and the relative velocity was observed for flames without a sooty tip. But the correlation was violated for flames with a sooty tip. As shown in **Figure S1**, the flame height measured from flame images with a sooty tip significantly deviate from the linear correlation between flame height and local velocity, which is followed in flames without a sooty tip. This shows that the flame boundary cannot be clearly identified in the presence of a sooty tip.

Due to the experimental limitations for performing highspeed OH* chemiluminescence and the effect of the sooty tip, the present experiment is confined to the parametric space where no such sooty bright yellow tip is observed in the wake flame. Hence, it is reasonable to conjecture that the soot contribution to luminescence is negligible in current experiments as the flame with a bright sooty tip is out of the scope of current experiments. So, it is reasonable to assume a minimal impact of the error on the flame height measurements due to sooting luminescence (which arises when OH* filter is not used). The current investigation primarily focuses on the qualitative aspects of the flame transitions and stabilization presented using simplified models to provide a framework for estimating the droplet flame response characteristics based on the externally imposed flow.

Figure S2: The experiments in our previous works show the vapor field emanating from a small region from the droplet wake, where the fuel vaporization occurs as it is exposed to the wake flame (Pandey et al. 2020; Vadlamudi et al. 2021). (a) Schlieren images of droplet wake flame, (b) PIV image obtained from the Mi-Scattering experiments by seeding the surrounding air (the central blank region shows the wake where fuel vaporises), (c) Fuel vapor in the wake illuminated by the scattering light from the light source, during flame imaging.
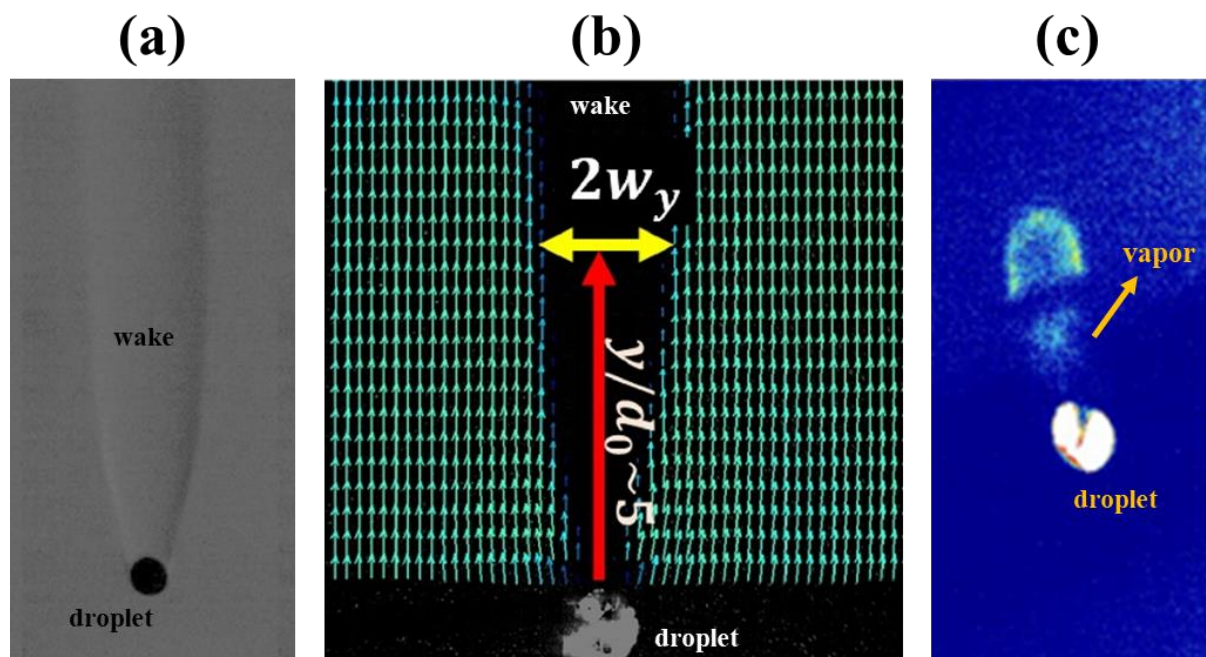
Figure S3: The data points represent the relation between flame height and relative velocity based on **Equation 3.3**, and the dotted line represents the linear fit for the data points in the range of $0.35 < \frac{h}{d} < 0.8$, showing that the linear approximation in **Equation 3.4** is a reasonable simplification of **Equation 3.3**.
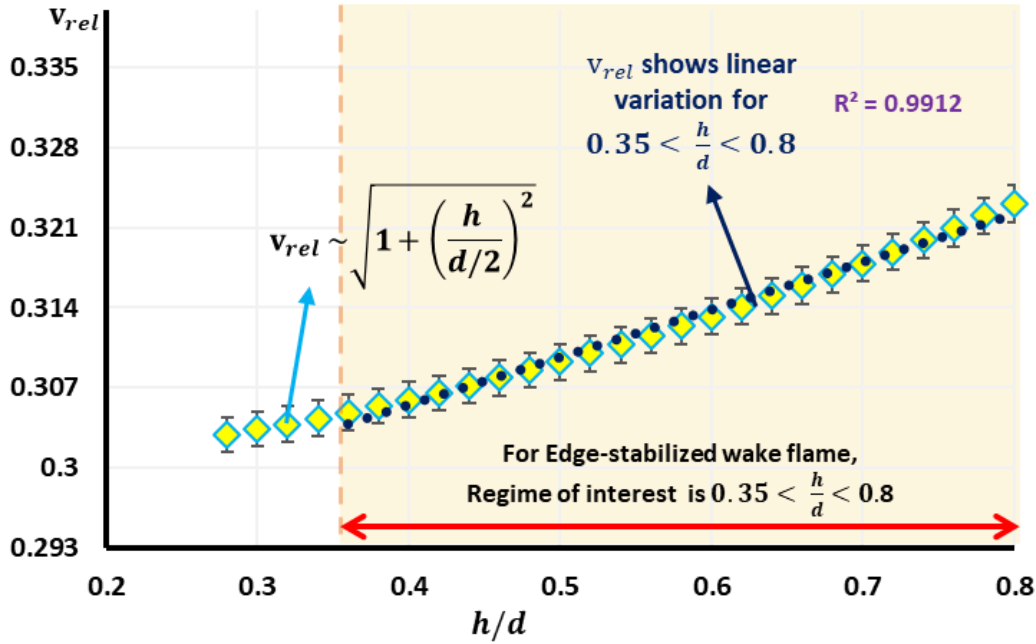
Equation 3.3 is used for edge-stabilized wake flame on a moving droplet and is only observed in a certain range of h/d, below which the flame structure changes as the wake flame tends to envelop the droplet. In the current experiments, the Edge-stabilized flame starts to change around $\frac{h}{d} \sim (0.35 - 0.2)$ and transitions into an enveloped flame as $\frac{h}{d} \longrightarrow 0$. Hence, the Edge-stabilized wake flame formulation is only valid for $\frac{h}{d} > 0.35$, where the flame exhibits a distinct Edge-stabilized structure. Moreover, the wake flame characteristics change for $\frac{h}{d} \sim 0.8$ (Re > 20), which leads to the transition of Edge-stabilized wake flame into a bluffbody stabilized flame at $\frac{h}{d} > 0.8$. Thus, in current experiments, **Equation 3.3** is only used for the range of $0.35 < \frac{h}{d} < 0.8$.

Equation 3.4 mentioned in the manuscript is a linear approximation of **Equation 3.3** in the range of the h/d values greater than $0.35 \left(\frac{h}{d} > 0.35 \right)$. To justify this linear approximation, the figure below plots **Equation 3.3** with h/d values on the abscissa. In the range of $0.35 < \frac{h}{d} < 0.8$ (where the Edge-stabilized flame structure is observed), the plot is observed to follow nearly a linear trend (shown in a navy dotted line) with an R^2-value tending to 1. This depicts that in the specified range, **Equation 3.3** follows a linear variation; hence, it can be approximated to be a linear proportionality relation, as shown in **Equation 3.4**.

**Figure S4:** Variation of normalized wake length against Re
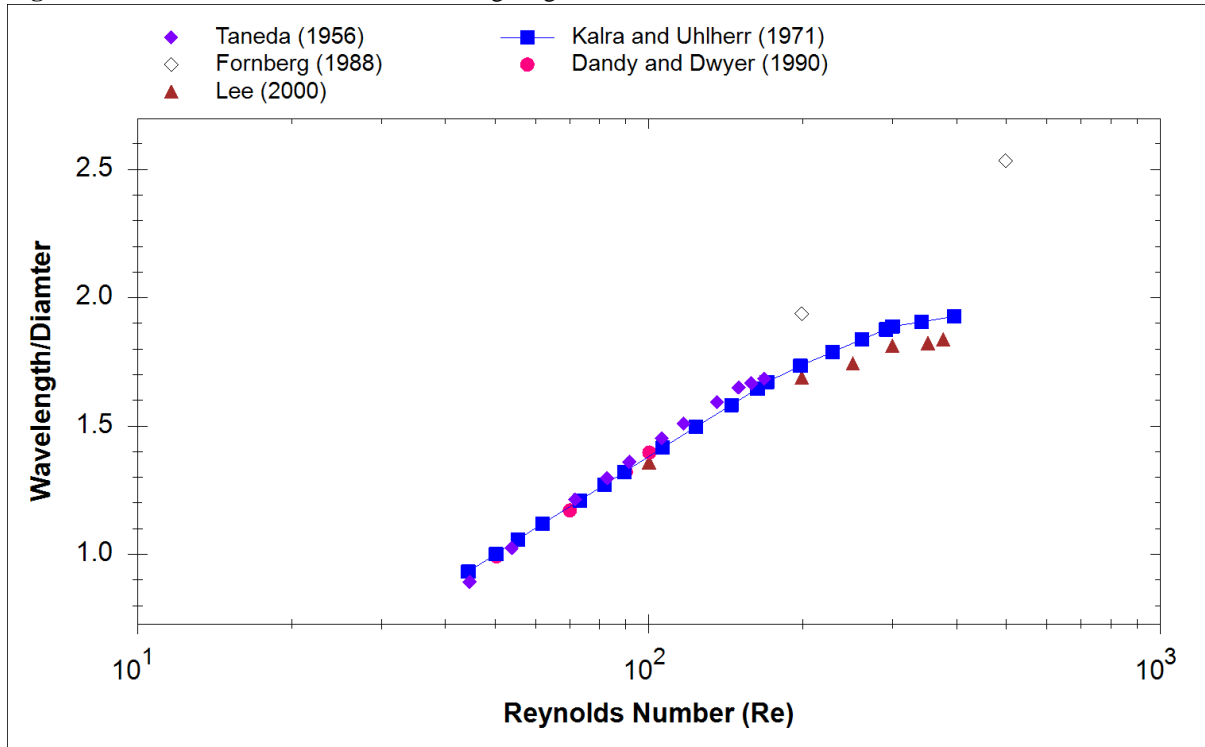
Results from the experimental and numerical studies (Kalra, T.R 1971; Taneda 1956; Fornberg 1988; Lee 2000; Dandy & Dwyer 1990) show that the wake length (defined as the distance up to which the wake region extends as measured from the droplet centre) varies linearly with the logarithm of the Reynolds number.

Identifying the flame structure from the flame images

From the visual shape of the flame and the geometry as depicted in Fig 3a and 6a of the manuscript, the Edge stabilized flames are dome-shaped or downward conical in shape, having a closed flame tip, as discussed in 3.2.1. The literature on the laminar lifted flame with a closed flame tip showed a similar dome-shaped flame structure for the edge flames (Jeon & Kim 2017; Van et al. 2018).

In case of bluffbody wake stabilized flames, the flame has an open tip (as shown by Pandey et al.) and has an open brush-like shape characterized by bright V-shaped flame fronts on either side (as shown in the Figure below). A detailed investigation has been performed by Pandey et al. on this flame structure using OH* chemiluminescence, high-speed Schlieren, and PIV measurements on the flow field around the droplet. It has been shown that the wake stabilized flame has an open tip with continuously decreasing equivalence ratio along the axial direction, due to entrainment. This leads to intermittent local extinction of the flame along the axial direction due to the lack of fuel availability. This was corroborated from the OH* chemiluminescence signature strength along the flame length, which shows a monotonic gradual decay along the axial direction (Pandey et al.).

Figure S5:
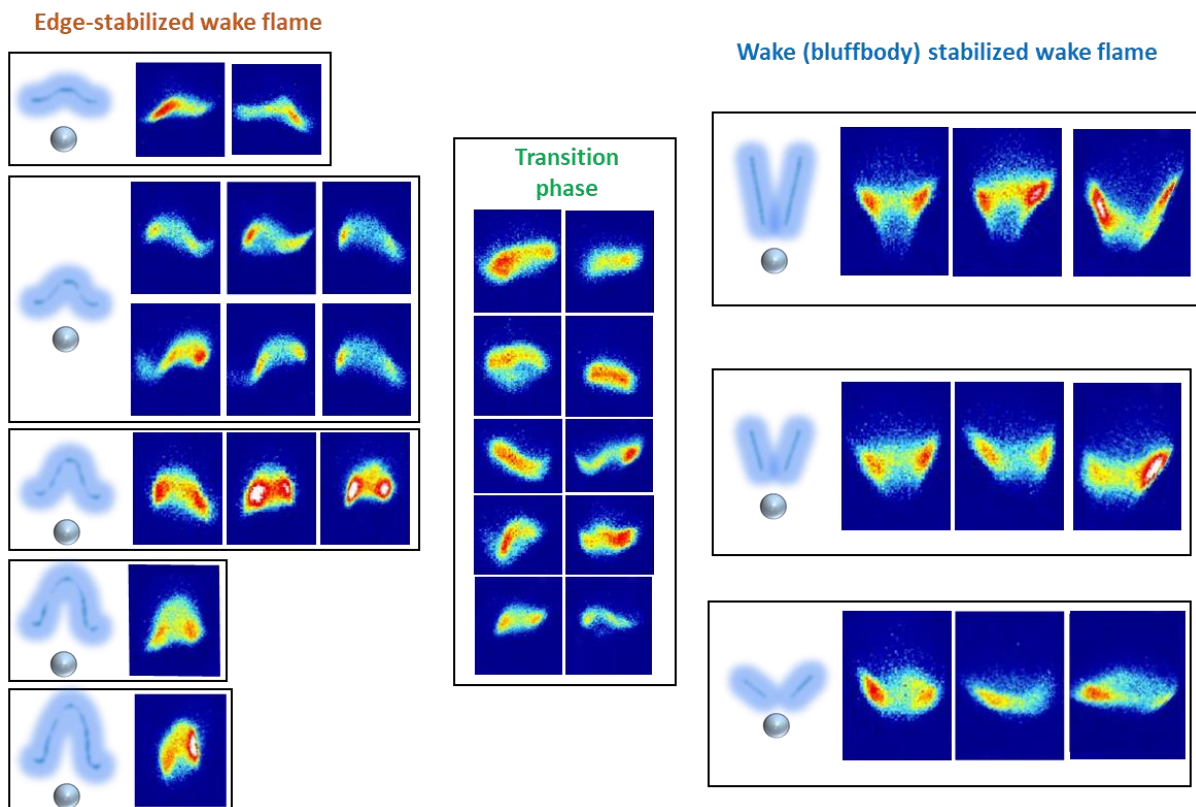
The Edge-stabilized wake flame, Transition phase, and the wake-stabilized flame shape have been depicted in the Figure. The reverse wake flame images have been rotated 180o in the upright position for simplicity. For each of the cases, left most image is the schematic of the flame shape, and equivalent experimental images from the current experiments have been depicted.

The Figure shows that except for the transition regime, where the flame shape is in an intermediate state as it is dynamically changing, the classification of such images is not possible. However, as shown in the Figure, the shape of the Edge-stabilized flames as well as the bluff body wake-stabilized flames from current experiments, are in good agreement with the literature.

REFERENCES

Dandy, D.S. & Dwyer, H.A. 1990 A sphere in shear flow at finite Reynolds number: effect of shear on particle lift, drag, and heat transfer. *J. Fluid Mech.* 216, 381–410.

Fornberg, B. 1988 Steady viscous flow past a sphere at high Reynolds numbers. *J. Fluid Mech.* 190, 471–489.

Jeon, M.-K. & Kim, N.I. 2017 Direct estimation of edge flame speeds of lifted laminar jet flames and a modified stabilization mechanism. *Combust. Flame* 186, 140–149.

Kalra, T.R, U., P.H.T. 1971 Properties of bluff body wakes. In Fourth Australian Conference on Hydraulics and Fluid Mechanics. Monash University, Melbourne, Australia.

Lee, S. 2000 Numerical study of the unsteady wake behind a sphere in a uniform flow at moderate Reynolds numbers. *Comput. Fluids* 29, 639–667.

Pandey, K., Basu, S., V, G., Potnis, A. & Chattopadhyay, K. 2020 Self-tuning and topological transitions in a free-falling nanofuel droplet flame. *Combust. Flame* 220, 144–156.

Taneda, S. 1956 Experimental investigation of the wake behind a sphere at low Reynolds numbers. *J. Phys. Soc. Jpn.* 11, 1104–1108.

Vadlamudi, G., Thirumalaikumaran, S.K. & Basu, S. 2021 Insights into the dynamics of wake flame in a freely falling droplet. *Phys. Fluids* 33, 123306.

Van, K.H., Jung, K., Yoo, C.S., Oh, S., Lee, B., Cha, M.S., Park, J. & Chung, S. 2018 Decreasing liftoff height behavior in diluted laminar lifted methane jet flames. *Proc. Combust. Inst.*